

# Evidence for a pseudogap in underdoped $\text{Bi}_2\text{Sr}_2\text{CaCu}_2\text{O}_{8+\delta}$ and $\text{YBa}_2\text{Cu}_3\text{O}_{6.50}$ from in-plane optical conductivity measurements

J. Hwang<sup>1,\*</sup>, J. P. Carbotte<sup>1,2</sup>, and T. Timusk<sup>1,2</sup>

<sup>1</sup>*Department of Physics and Astronomy, McMaster University, Hamilton, Ontario L8S 4M1, Canada and*

<sup>2</sup>*The Canadian Institute for Advanced Research, Toronto, Ontario M5G 1Z8, Canada*

(Dated: August 22, 2021)

The real part of the in-plane optical self-energy data in underdoped  $\text{Bi}_2\text{Sr}_2\text{CaCu}_2\text{O}_{8+\delta}$  (Bi-2212) and ortho II  $\text{YBa}_2\text{Cu}_3\text{O}_{6.5}$  contains new and important information on the pseudogap. Using a theoretical model approach we find that the density of state lost below the pseudogap  $\Delta_{pg}$  is accompanied with a pileup just above this energy. The pileup along with a sharp mode in the bosonic spectral function leads to an unusually rapid increase in the optical scattering rate and a characteristically sloped peak in the real part of the optical self-energy. These features are not found in optimally doped and overdoped samples and represent a clearest signature so far of the opening of a pseudogap in the in-plane optical conductivity.

PACS numbers: 74.25.Gz, 74.62.Dh, 74.72.Hs

A striking feature of the underdoped cuprates, not present in conventional metals, is the appearance of a pseudogap[1] below a characteristic temperature  $T^*$ . In general, the opening of a pseudogap  $\Delta_{pg}$  leads to a reduction in the electronic density of states (DOS) around the Fermi energy. Since, as yet, there is no full understanding of the exact origin of the pseudogap in the cuprates, an important issue is how it should be modelled, its width in frequency, its behavior as a function of doping and temperature and what happens to the spectral weight in the gap. While the first evidence of a pseudogap in the cuprates came from NMR experiments[2, 3] that showed a gap in the spin excitation spectrum, a gap in the charge excitations was found in the  $c$ -axis conductivity of underdoped YBCO by Homes *et al.*[4]. The conductivity in this direction is incoherent, and like  $c$ -axis tunneling, is expected to be proportional to the density of states. Homes *et al.* concluded that the spectral weight lost in the pseudogap region was recovered at much higher frequencies. A similar conclusion was reached by Loram *et al.* from specific heat measurements [5]. In contrast, Yu *et al.* from a recent study of  $c$ -axis conductivity of underdoped  $\text{RBa}_2\text{Cu}_3\text{O}_{6.5}$  (R=Y, Nd, and La) extending the measurements to higher frequency found that spectral weight was recovered [6]. Also tunneling data suggests that the "coherence peak" that signals a tunneling conductance that is enhanced over the background persists well into the normal state in Bi-2212 [7] suggesting a recovery of gapped states.

The pseudogap is more difficult to identify in the ab-plane transport. While it was clear very early on that the ab-plane absorption showed an unmistakable decrease at energies below  $\Delta_{pg}$ [8, 9, 10, 11, 12], a clear interpretation in terms of a pseudogap was problematic since it is difficult to separate the effects of a pseudogap (a pseudogap in the density of states) and a gap in the spectrum of inelastic excitations (a spin gap) since both reduce absorption at low frequencies. Further, studies of the real

part of the conductivity did not show the expected reduction in optical spectral weight below the pseudogap energy[13]. This remains unexplained. In this letter we find that by focussing not on features in the optical conductivity, but on the real and imaginary parts of the optical self-energy we *are able to* separate the contributions of the pseudogap and inelastic scattering. Furthermore, simulations with simple models show that spectral features in the density of states are less spread out in the self-energy than in the conductivity making small changes easier to estimate accurately. We can trace to missing states below the gap to the region just above it.

It has become common in the optical literature to analyze reflectivity measurements in terms of the real and imaginary parts of the optical conductivity  $\sigma(\omega) = \sigma_1(\omega) + i\sigma_2(\omega)$  and present the results for the optical scattering rate  $1/\tau^{op}(\omega)$  as a function of  $\omega$ . The extended Drude formula, which is valid for correlated electrons, can be written as  $4\pi\sigma(\omega) \equiv i\omega_p^2/[\omega - 2\Sigma^{op}(\omega)]$ , where  $\omega_p$  is the plasma frequency and  $\Sigma^{op}(\omega) \equiv \Sigma_1^{op}(\omega) + i\Sigma_2^{op}(\omega)$  is by definition the optical self-energy. Its imaginary part gives the optical scattering rate and its real part is related to the optical mass re-normalization. The real and imaginary parts of  $\Sigma^{op}(\omega)$  are related by Kramers-Kronig (K-K) transformations. They play, for the optical conductivity, a role similar to that played by the quasiparticle self-energy  $\Sigma^{qp}(\omega)$  in angle-resolved photoemission spectroscopy but these are different quantities although they are closely related [14, 15].

The real part of  $\Sigma^{op}(\omega)$  obtained from the in-plane conductivity in the highly underdoped regime[12, 16, 17] shows a particularly clear and striking signature of the pseudogap modelled just as was done from the specific heat[5] by a simple reduction in electronic density of states in the vicinity of the Fermi energy. Contrary to the specific heat case, however, we find evidence that these missing states in DOS pile up in the region just above the pseudogap energy. While the exact shape taken by

the quasiparticle DOS around the Fermi energy will in principle be reflected in the shape of the real part of the optical self-energy, these details are of secondary importance.

In Fig. 1 we compare results for  $-2\Sigma_1^{op}(\omega)$  vs.  $\omega$  obtained in ref. [16, 17] for an underdoped Bi-2212 sample (top frame) with an overdoped sample with approximately the same critical temperature (bottom frame). The evolution of the curves seen as the temperature is lowered is quite different in the two cases. The overdoped samples show only small changes while the underdoped one shows the growth of a sharp triangle-like peak around  $750\text{ cm}^{-1}$ . We will argue that this sharp peak is a result of a pseudogap opening with a recovery region just above it while at the same time a sharp resonance exists in the electron-boson spectral density  $I^2\chi(\omega)$  which we believe to be due to spin fluctuations and not phonons. The inset in the top frame of Fig. 1 shows results from the highly underdoped ortho II compound  $\text{YBa}_2\text{Cu}_3\text{O}_{6.5}$ [12] in which every second chain is full and the others are empty, leading to a perfect stoichiometric sample. The same characteristic temperature evolution is seen in YBCO as in Bi-2212. This suggests that this sharp peak is a universal feature of the underdoped cuprates.

To establish our central point it will be sufficient to use approximate, but surprisingly accurate, formulas that relate the real and imaginary parts of the scattering rates to the electron-boson spectral density  $I^2\chi(\omega)$  for zero temperature from the work of Mitrovic *et al.*[18] and others[19, 20, 21, 22]. At  $T = 0$  we have[18],

$$-2\Sigma_1^{op}(\omega) \cong \frac{2}{\omega} \int_0^\infty d\Omega I^2\chi(\Omega) \int_0^\infty d\omega' \tilde{N}(\omega') \times \ln \left| \frac{(\omega' + \Omega)^2}{(\omega' + \Omega)^2 - \omega^2} \right|$$

$$-2\Sigma_2^{op}(\omega) \cong \frac{1}{\tau^{op}(\omega)} \cong \frac{2\pi}{\omega} \int_0^\omega d\Omega I^2\chi(\Omega) \int_0^{\omega-\Omega} d\omega' \tilde{N}(\omega')$$

where  $\tilde{N}(\omega)$  is the renormalized electronic density of states symmetrized about the Fermi energy. It contains the pseudogap and, for finite bands, would decay rapidly at the renormalized band edge. There is a cutoff frequency,  $\Omega_c$  on the spectral density. Here we used  $\Omega_c = 4000\text{ cm}^{-1}$ .

We begin with the following observation. For a constant density of states and coupling to a single mode of energy  $\omega_E$  *i.e.*  $I^2\chi(\omega) = A_0\delta(\omega - \omega_E)$  with  $A_0$  setting the scale, the optical scattering rate ( $1/\tau^{op}(\omega)$ ) is zero for  $\omega < \omega_E$  and equal to  $2\pi A_0[(\omega - \omega_E)/\omega]$  for  $\omega \geq \omega_E$  which starts from zero at  $\omega = \omega_E$  and saturates to  $2\pi A_0$  only for  $\omega \gg \omega_E$ . If, in addition, there is a full gap  $\Delta_{pg}$  (the pseudogap) in the symmetrized density of electronic states  $\tilde{N}(\omega)$ ,  $1/\tau^{op}(\omega)$  starts instead

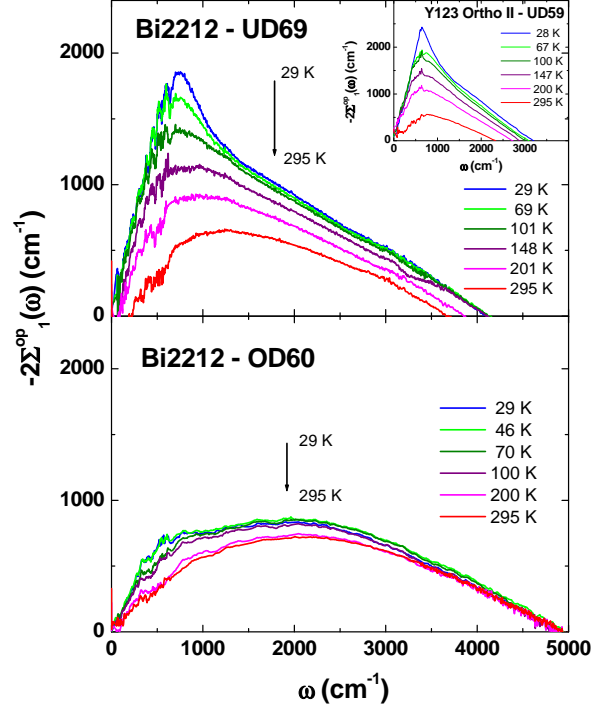


FIG. 1: (color online) Minus twice the real part of the optical self-energy  $-2\Sigma_1^{op}(\omega)$  vs.  $\omega$  for underdoped (top frame) and overdoped Bi-2212 (bottom frame)[16, 17]. The inset shows the corresponding results for underdoped ortho II YBCO[12].

from zero at  $\omega = \omega_E + \Delta_{pg}$  and rise towards saturation according to the modulating factor  $(\omega - \omega_E - \Delta_{pg})/\omega$  which effectively rises more slowly with  $\omega$  than does  $(\omega - \omega_E)/\omega$ . This is seen in the middle frame of Fig. 2 where we show  $-2\Sigma_2^{op}(\omega)$  for three cases, A, B, C all based on the electron-boson spectral density shown in the inset,  $I^2\chi(\omega) = A_p/[\sqrt{2\pi}(d/2.35)]e^{-(\omega-\omega_p)^2/[2(d/2.35)^2]} + A_s\omega/[\omega_{sf}^2 + \omega^2]$ , where  $A_p = 200$ ,  $\omega_p = 250\text{ cm}^{-1}$ ,  $d = 10\text{ cm}^{-1}$ ,  $A_s = 100\text{ cm}^{-1}$ , and  $\omega_{sf} = 500\text{ cm}^{-1}$ . It has a peak at  $\omega = 250\text{ cm}^{-1}$  and a broad background extending to  $4000\text{ cm}^{-1}$ , modelled on results for underdoped ortho II YBCO[12]. The curve A includes no pseudogap while curve B has  $\Delta_{pg} = 550\text{ cm}^{-1}$  and starts from zero at  $800\text{ cm}^{-1}$  in contrast to curve A which starts at  $250\text{ cm}^{-1}$ . Comparing with curve A shows that a pseudogap leads to an optical scattering rate which rises less steeply from zero than it would with  $\Delta_{pg} = 0$ . A slower rise would also arise if instead of using a delta function at  $\omega_E$  for  $I^2\chi(\omega)$  part of the weight (not shown here) was distributed to a region of higher frequencies. The two curves for  $-2\Sigma_2^{op}(\omega)$  as well as C continue to rise at the largest photon energies shown because we have included a background in  $I^2\chi(\omega)$  which extends to  $4000\text{ cm}^{-1}$ . The curve C includes a full pseudogap just as in curve B but now it is also assumed that the lost states in  $\tilde{N}(\omega)$  reappear just above  $\Delta_{pg}$  in the interval  $\Delta_{pg}$  to  $2\Delta_{pg}$ .

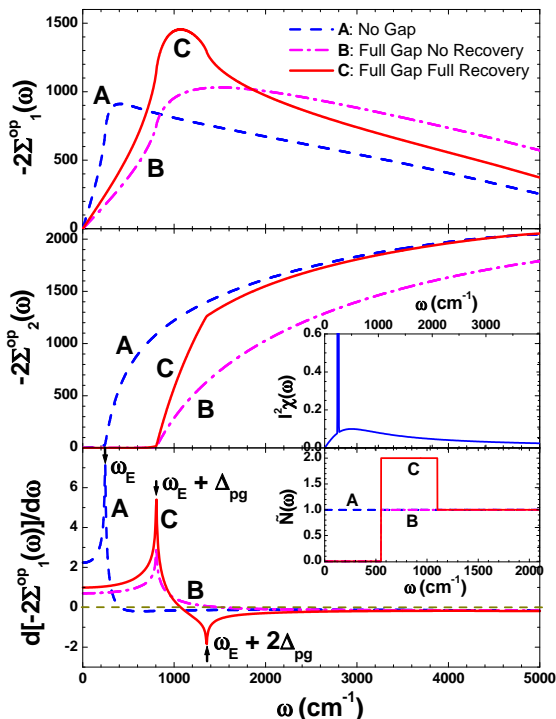


FIG. 2: (color online) Model results for  $-2\Sigma_1^{op}(\omega)$  vs.  $\omega$  (top frame) and  $-2\Sigma_2^{op}(\omega)$  vs.  $\omega$  (middle frame). The electrons are coupled to bosons with electron-boson spectral weight shown in the inset of the middle frame. A, B and C curves are with no pseudogap, pseudogap without recovery region, and pseudogap with recovery, respectively. The corresponding density of states,  $\tilde{N}(\omega)$ , is shown in the inset (bottom frame) with the same line types. In the bottom frame we show the derivative,  $d[-2\Sigma_1^{op}(\omega)]/d\omega$  vs.  $\omega$ .

These extra electronic states lead to increased scattering and the curve C rises from zero much more rapidly than curve B. Also at the energy marking the end of the enhanced density of states (recovery region) there is a kink in  $1/\tau^{op}(\omega)$  beyond which the rate of increase in  $1/\tau^{op}(\omega)$  becomes less rapid.

In the top frame of Fig. 2 we show the real part of  $\Sigma^{op}(\omega)$  which corresponds to the K-K transformation of the optical scattering rates of the middle frame. For the curve A there is no singularity at  $\omega_E$ . Rather there is a very broad maximum at  $\omega \sim \sqrt{2}\omega_E$  followed by a slow drop to about 1/3 its maximum value at  $4000 \text{ cm}^{-1}$ . If, on the other hand, we include a pseudogap without a recovery region above it, we get curve B, for which the peak falls at  $\sim \sqrt{2}(\omega_E + \Delta_{pg})$ . Including a recovery region in the density of states changes the shape of  $\Sigma_1^{op}(\omega)$  significantly as we can see in curve C. Here we include a full gap below  $\Delta_{pg}$  and displaced states just above as shown in the solid (red) curve of the inset on the bottom panel of Fig. 2 where our model  $\tilde{N}(\omega)$  is shown. In this cases  $-2\Sigma_1^{op}(\omega)$  develops a much more pronounced peak between  $\omega_E + \Delta_{pg}$  and  $\omega_E + 2\Delta_{pg}$ , points marked

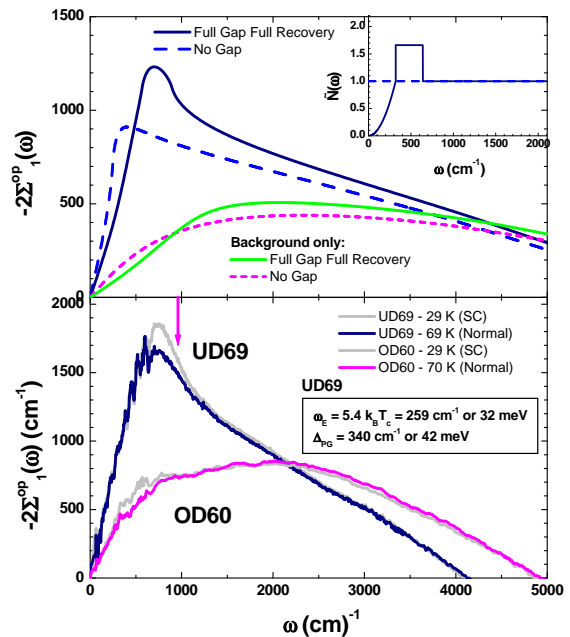


FIG. 3: (color online) Comparison of  $-2\Sigma_1^{op}(\omega)$  vs.  $\omega$  for underdoped Bi-2212 and overdoped Bi-2212 samples, bottom frame. The top frame shows results of model calculations. Solid (dark-blue) and dashed (blue) curves are with pseudogap and recovery and without gap (see corresponding quadratic behavior  $\tilde{N}(\omega)$  curves in the inset) for the  $I^2\chi(\omega)$  shown in the inset to Fig. 2. Dashed (purple) and solid (green) curves are obtained when the electron-boson spectral density, just has a continuous background.

by maximum slopes. This structure is seen both in underdoped Bi-2212 and YBCO samples at low temperature normal state of Fig. 1 and is strong evidence for a pileup of the spectral weight lost below  $\Delta_{pg}$ , in the region  $\Delta_{pg} < \omega < 2\Delta_{pg}$ . The above characteristics are a clear signature of pseudogap formation in the in-plane conductivity.

The feature of the model curves displayed in the top frame of Fig. 2 which we have just described and which are most important for the interpretation of experiments, shows up even more clearly in the *derivative* of the real part of the optical self-energy  $d[-2\Sigma_1^{op}(\omega)]/d\omega$ . Results are shown in the bottom panel of Fig. 2. The curve A shows maximum slope at the energy  $\omega_E$  of the peak in  $I^2\chi(\omega)$  (see inset in the middle frame of Fig. 2) and it is zero at  $\sim \sqrt{2}\omega_E$ . Curve B has a maximum at  $\omega_E + \Delta_{pg}$  and a zero at  $\sim \sqrt{2}(\omega_E + \Delta_{pg})$  while curve C peaks at  $\omega_E + \Delta_{pg}$  and shows a minimum at  $\omega_E + 2\Delta_{pg}$  indicating the end of the recovery region in our model of the effective electronic density of states,  $\tilde{N}(\omega)$ .

In the lower panel of Fig. 3 we repeat our experimental results for the underdoped and overdoped samples of Fig. 1 but for clarity, show only the two lowest temperatures. In the top frame we show four curves. One set is based on the electron-boson spectral density shown in

the inset of Fig. 2. The other is obtained when only the background is

kept in  $I^2\chi(\omega)$ . In Bi-2212 series we have found that in the overdoped regime there is no prominent peak in the electron-boson spectral density, only a background remains[14, 15, 23, 24]. For this figure we have used quadratic pseudogap shown as the (dark-blue) solid curve in the inset of Fig. 3. Starting with the two curves for the background only,  $I^2\chi(\omega) = 100\omega/[500^2 + \omega^2]$ , we see that including a pseudogap does not change the curve for  $\Sigma_1^{op}(\omega)$  much in agreement with the data and there is, in this sense, no clear signature of  $\Delta_{pg}$  in such spectra. On the other hand contrasting with the other two curves, the pseudogap now clearly changes the shape of  $\Sigma_1^{op}(\omega)$  and brings it much closer to the experimental results for the underdoped sample (lower panel). The peak in the (dark-blue) solid curve can be made sharper and resemble even more a logarithmic singularity by decreasing the width of the recovery region. This arises because the sharp rise seen in  $1/\tau^{op}(\omega)$  (curve B) of Fig. 2 middle frame, can be made even steeper and come closer to a pure vertical rise. We conclude that the striking difference observed in  $\Sigma_1^{op}(\omega)$  between underdoped and overdoped samples can be understood to result from the absence of a pseudogap and a sharp peak in  $I^2\chi(\omega)$  for the overdoped case, and a combination of a peak and pseudogap in the underdoped case. Both are needed to get agreement with the data, including a recovery of spectral weight in the electronic density of states in the region just above the pseudogap with the end of the recovery region marked by a kink in  $\Sigma_1^{op}(\omega)$  around  $940\text{ cm}^{-1}$  for Bi-2212 (purple arrow in lower panel of Fig. 3) and similarly  $970\text{ cm}^{-1}$  for YBCO. If we assume the position of the peak in  $I^2\chi(\omega)$  to be set by the neutron resonance energy given by  $\Omega_{res} = 5.4k_B T_c$  [25] we conclude that the pseudogap has a value of 43 meV in Bi-2212 and nearly the same 45 meV in YBCO and that the recovery region is approximately  $\Delta_{pg}$  wide. We note that our suggestion that the recovery of spectral weight occurs immediately above the gap region in the normal state just above  $T_c$ , is in accord with tunneling spectra [7].

In summary, the real part of the optical self-energy,  $-2\Sigma_1^{op}(\omega)$ , defined through a generalized Drude formula at low temperature in the normal state, for the underdoped case, shows characteristic triangular behavior around  $750\text{ cm}^{-1}$  not seen in overdoped samples. This behavior is traced to the existence of a pseudogap  $\Delta_{pg}$  in the electronic density of states with states lost below  $\Delta_{pg}$  recovered in the region immediately above it as well as the existence of a peak in the electron-boson spectral density responsible for the inelastic scattering. By contrast, in the overdoped samples no pseudogap opens and the fluctuation spectrum  $I^2\chi(\omega)$  has no resonance peak but rather consists only of a reasonably flat background. Criteria to recover a value of the pseudogap and the end

of the recovery region are given and applied to underdoped Bi-2212 and ortho II YBCO. The signature of the pseudogap is much clearer in the optical self-energy than it is in the in-plane conductivity, the quantity used in previous studies.

This work has been supported by the Natural Science and Engineering Research Council of Canada (NSERC) and the Canadian Institute for Advanced Research (CIAR). We acknowledge the contribution of Hiroshi Eisaki and Genda Gu for the Bi-2212 crystals and Ruixing Liang, Doug Bonn, and Walter Hardy for the YBCO crystal.

---

\* Electronic address: jhwang@phys.ufl.edu

- [1] T. Timusk and B. Statt, Rep. Prog. Phys. **62**, 61 (1999).
- [2] W. W. Warren Jr. *et al.*, Phys. Rev. Lett. **62**, 1193 (1989).
- [3] H. Alloul, T. Ohno, and P. Mendels, Phys. Rev. Lett. **63**, 1700 (1989).
- [4] C. C. Homes, T. Timusk, R. Liang, D. A. Bonn, and W. N. Hardy, Phys. Rev. Lett. **71**, 1645 (1993).
- [5] J. W. Loram Mirza, K. A. Mirza, J. R. Cooper, J. L. Tallon, J. Phys. Chem. Solids **59**, 2091 (1998).
- [6] Li Yu *et al.*, preprint cond-mat/0705.0111.
- [7] Ch. Renner, B. Revaz, J-Y Genoud, K. Kadowaki, and O. Fischer, Phys. Rev. Lett. **80** 149, (1998).
- [8] J. Orenstein *et al.*, Phys. Rev B **42**, 6342 (1990).
- [9] L.D. Rotter *et al.*, Phys. Rev. Lett. **67**, 2741 (1991).
- [10] D. N. Basov *et al.*, Phys. Rev. Lett. **77**, 4090 (1996).
- [11] A. V. Puchkov, D. N. Basov, and T. Timusk, J. Phys.: Condens. Matter **8**, 10049 (1996).
- [12] J. Hwang *et al.*, Phys. Rev. B **73**, 014508 (2006).
- [13] A. F. Santander-Syro, R. P. Lobo, N. Bontemps, Z. Konstantinovic, Z. Li, and H. Raffy, Phys. Rev. Lett. **88**, 097005 (2002).
- [14] J. P. Carbotte, E. Schachinger, and J. Hwang, Phys. Rev B **71**, 054506 (2005).
- [15] E. Schachinger, J. J. Tu, and J. P. Carbotte, Phys. Rev B **67**, 214508 (2003).
- [16] J. Hwang, T. Timusk, and G. D. Gu, Nature (London) **427**, 714 (2004).
- [17] J. Hwang, T. Timusk, and G. D. Gu, J. Phys.: Condens. Matter **19**, 125208 (2007).
- [18] B. Mitrovic and M. A. Fiorucci, Phys. Rev. B **31**, 2694 (1985).
- [19] P. B. Allen, Phys. Rev. B **3**, 305 (1971).
- [20] S.V. Shulga, O.V. Dolgov, and E.G. Maksimov, Physica C **178**, 266 (1991).
- [21] S. G. Sharapov and J. P. Carbotte, Phys. Rev. B **72**, 134506 (2005).
- [22] A. Knigavko and J. P. Carbotte, Phys. Rev. B **72**, 035125 (2005); *ibid* **73**, 125114 (2006).
- [23] E. Schachinger, D. Neuber, and J. P. Carbotte, Phys. Rev. B **73**, 184507 (2006).
- [24] J. Hwang, T. Timusk, E. Schachinger, and J. P. Carbotte, Phys. Rev. B **75**, 144508 (2007).
- [25] H. He *et al.*, Phys. Rev. Lett. **86**, 1610 (2001).